Rapid Communication

Tailoring the plasmonic properties of gold-liposome nanohybrids as a potential powerful tool for light-mediated therapies

Marta Rubio-Camacho [a,b], María José Martínez-Tomé [a], Carlos Cuestas-Ayllón [b], Jesús M. de la Fuente [b,c], Rocío Esquembre [a,*], C. Reyes Mateo [a,*]

[a] *Instituto de Investigación, Desarrollo e Innovación en Biotecnología Sanitaria de Elche (IDiBE), Universidad Miguel Hernández (UMH), Elche, Alicante, Spain*
[b] *Instituto de Nanociencia y Materiales de Aragón (INMA), Consejo Superior de Investigaciones Científicas (CSIC) & University of Zaragoza, Zaragoza, Spain*
[c] *Centro de Investigación Biomédica en Red de Bioingeniería, Biomateriales y Nanomedicina (CIBER-BBN), Instituto de Salud Carlos III, Madrid, Spain*

ARTICLE INFO

ABSTRACT

A fast and environmentally-friendly methodology has been developed by in situ synthesis of gold nanoparticles (AuNPs) on thermosensitive liposomes in different phase-states, obtaining nanohybrids with controllable and tunable plasmon modes within the visible/near-infrared region. Lipid phase, charge and synthesis temperature influence the final arrangement of AuNPs, so when the synthesis is performed on zwitterionic liposomes in fluid phase, discrete AuNPs with plasmon peaks in the visible region are obtained, while in gel phase AuNPs tend to aggregate forming nanoclusters, leading to plasmon bands gradually shifted to the infrared as the synthesis temperature decreases. The formed nanohybrids retain the physical properties of the liposomes (fluidity, degree of hydration, cooperativity) by maintaining the transition temperature in the mild-hyperthermia range, while preserving their light-to-heat conversion properties. Therefore, these nanohybrids can be considered excellent candidates as versatile photothermal agents with controlled drug delivery capacity, being powerful tools for light-mediated therapies.

1. Introduction

Gold nanoparticles (AuNPs) as a result of the localized surface plasmon resonance (LSPR) effect can absorb light from the red to the infrared region and dissipate it into the surrounding environment in the form of heat [1]. Their unique thermal and optical properties, together with the excellent biocompatibility, inert nature and easy surface functionalization, have made these nanoparticles excellent platforms for a wide range of applications in diverse fields, including catalysis, bioimaging, sensing and detecting, therapeutics, optoelectronic, photovoltaic and energy storage [2–7]. Regarding therapeutic applications, one of their most promising uses is photothermal therapy (PTT), especially in cancer treatment, due to their high light-to-heat conversion efficiency [1]. AuNPs preferentially accumulate in tumor tissues as a consequence of the enhanced permeability and retention effect, where are irradiated at the wavelength of the plasmon band, producing heat locally and causing cancer cell death. This means that the photothermal heat generated by AuNPs is almost tumor-specific with an excellent spatio-temporal resolution and thus avoiding the side effects of traditional hyperthermia [8–10].

Tuning the LSPR band of AuNPs to the near-infrared (NIR) region is desirable in many of their applications. For several years now, great efforts have been made in this direction in order to obtain gold nanostructures with NIR plasmonic modes and to find tools that enable their control [11–13]. To modulate the position of this band, the most common alternative is to modify the final shape and size of the nanoparticle or its surface by means of the synthesis strategy. While the maximum absorption spectrum for regular spherical colloidal Au is around 510–530 nm (red color solutions), when anisotropy is added to the nanoparticle - such as the growth of nanorods, nanoprisms or nanostars-the AuNPs obtained, having different length-to-width ratios, create different colored solutions as a consequence of changes in their reaction with light [14–16]. This phenomenon is mainly due to the split that LSPR band suffers into two different plasmon bands: a strong one in the NIR region, corresponding to electron oscillations in the longitudinal axis, and a weak one in the UV–Visible, corresponding to electron oscillations in the transversal axis [1,8,17]. For biomedical applications, such a shift allows irradiating the tissues in the NIR, which has much

greater body transparency and lower energy, making it preferable for PTT. However, some of the methods to produce anisotropic AuNPs rely on difficult syntheses with complex approaches, many of which use cetyltrimethylammonium bromide (CTAB), a highly cytotoxic surfactant, as a mediator, limiting their use in biomedical applications [15]. In this regard considerable efforts are currently being made to develop "go green" approaches and bioinspired methodologies to overcome these drawbacks [15,18,19].

Another approach to shift the plasmon band of AuNPs into the NIR region is to induce their aggregation or coalescence, giving rise to new collective properties that are not observed in isolated particles [12,20]. This is because the surface plasmon oscillation in the metal nanoparticles changes drastically when they are densely packed. The shortening of the interparticle distance, leads to a collective plasmon oscillation of the aggregated system resulting in a strong dipole-dipole interaction, which causes the LSPR band to shift from the 520 nm to 750–800 nm, turning the color of the suspension blue. This effect also causes the absorption band broadening, as the spectrum is a composite of the conventional LSPR due to spherical nanoparticles and the new peak due to interparticle interactions [21].

Synthesis strategies for obtaining AuNPs clusters include mainly two approaches: aggregation of already formed AuNPs or *in situ* formation. For the first approach, AuNPs are usually prepared by Turkevich's method, through citrate reduction of $HAuCl_4$ at 100 °C [22]. Once prepared, aggregation can be triggered by replacing the charged species on the surface with oppositely charged or uncharged adsorbates, by changing pH and/or temperature, by irradiation, by adding salts or by increasing the concentration to decrease the interparticle distance [23]. However, while the addition of polymers can help stabilize these aggregates [24], most of these approaches usually exhibit poor controllability and reproducibility since result in randomly formed polydisperse aggregates which often precipitate and cause the solution to become colorless.

The formation of gold aggregates can also take place by generating AuNPs *in situ*, in the presence of a reducing agent and a supporting element. Aggregation occurs mainly through electrostatic interactions between such an element and the nascent AuNPs during their formation and growth process [21]. The binding between the particles and the support generally relies on the attractive coulomb forces between the negatively charged AuNPs or their precursors and the positively charged groups of the support [25]. An example of this strategy is the use of liposomes as supporting elements, so that the AuNPs aggregates are obtained *in situ* on the lipid membrane. The formation of these complexes increases the functionality of both AuNPs and liposomes resulting in hybrid nanoplatforms that combine properties of contrast agent, controlled-release drug carrier and PTT activity. Troutman et al. designed gold-coated liposomes capable of releasing their contents when irradiated at the wavelength of the LSPR band, due to the increase in bilayer permeability induced by the heat generated during the process. The position of the plasmon band could be tuned by modifying the amount of reduced gold, which resulted in aggregates that shifted the LSPR to the NIR [26]. In addition to this work, further studies have shown that the degree of aggregation of AuNPs on giant liposomes surface can be controlled not only by changing the amount of gold precursor but also the liposome charge and composition [27].

In the works mentioned above, the *in situ* synthesis of AuNPs on the liposome surface is performed at room temperature, without taking into account the role played in this process by parameters such as the physical state of the bilayer or the synthesis temperature. In fact, lipids can exist in a variety of lamellar phases depending on temperature, which could influence nanoparticle formation. To our knowledge, this type of study has not been performed before for *in situ* synthesis, and may be useful to know to what extent, by modifying these parameters, it is possible to modulate the formation of the AuNPs and, consequently, the position of the plasmon band. In the present work, we have explored this issue, finding clear relationships between the packing degree of the

lipid bilayer and the clustering of AuNPs. In addition, we have studied to what extent these aggregates modify the properties of the bilayer and its thermotropic behavior. For this purpose, we have used thermosensitive liposomes composed of 1,2-dipalmitoyl-sn-glycero-3-phospho-rac-(1-glycerol) sodium salt (DPPG) and 1,2-dipalmitoyl-sn-glycero-3-phosphocholine (DPPC). These lipids undergo a gel-to-fluid phase transition at a temperature several degrees above physiological temperature ($T_m \sim 42$ °C), passing from a state in which the lipids are highly packed in the bilayer, to one in which the degree of fluidity and permeability increases considerably [28]. These lipids have been selected for two reasons: on the one hand, because they allow for easily switch the physical state of the bilayer and thus explore to what extent the lipid phase plays a role in the *in situ* synthesis of AuNPs. On the other hand, because their applicability in nanomedicine, as these liposomes are able to transport drugs and release them in a controlled manner at mild hyperthermia temperatures (41–44 °C). Such temperatures increase tumor perfusion, improve drug uptake and make cancer cells temporarily sensitive to other treatments [29].

To make the synthesis of nanohybrids as environmentally friendly as possible, we used ascorbic acid as a reducing agent. Its use has many advantages, especially when applied in biomedicine, because unlike the more frequently Turkevich's method, it does not require high temperatures so that the synthesis can be performed *in situ*, without damaging the liposomes [30]. In addition, the nanoparticles obtained meet the requirements of chemical cleanliness, as opposed to other methods that use CTAB during the synthesis process.

2. Materials and methods

The chemical reagents used for the synthesis of nanohybrids and for their characterization, are described in the Supporting Information.

Multilamellar vesicles (MLVs) were prepared from lipid solutions of DPPC, DMPC, and DPPG using the thin-film hydration method. Then large unilamellar vesicles (LUVs) were obtained from the MLVs solutions by pressure extrusion. AuNPs were synthesized in presence of LUVs at different temperatures, obtaining AuNP@lipid nanohybrids, as described in the Supporting Information.

The hydrodynamic size of liposomes, AuNPs and AuNP@lipid nanohybrids was analyzed by Dynamic Light Scattering (DLS) technique. Both the morphology and location of AuNPs in the nanohybrids synthesized at different temperatures, were characterized by electron microscopy. LSPR bands of AuNPs and AuNP@lipid nanohybrids were analyzed using UV–Visible spectroscopy. The steady-state fluorescence anisotropy $<r>$ and the time-resolved fluorescence measurements of the probe diphenylhexatriene (DPH), incorporated in DPPC LUVs and AuNP@DPPC nanohybrids synthesized at different temperatures, allowed studying the physical properties of the bilayer. The photothermal conversion was studied by measuring the sample's temperature variation over time under NIR laser irradiation (1064 nm). Detailed information on the methods can be found in the Supporting Information.

3. Results and discussion

3.1. Synthesis of AuNPs in water as a function of temperature

As a previous step to the synthesis of AuNPs on lipid membranes, we explored to what extent the temperature and the amount of Au precursor influenced the LSRP properties of the nanoparticles obtained in water. AuNPs were prepared at 22 °C, as is described in Materials and Methods. The sample quickly turned reddish in color and its absorption spectrum showed a maximum at 525 nm, which coincides with the expected wavelength for spherical AuNPs of nanometric size (Figs. 1 and S1). The resulting AuNPs were subsequently characterized by DLS obtaining a single population with a hydrodynamic diameter around 33 nm and a PDI of 0.196. Regarding the morphology, samples were prepared and observed under FESEM in STEM mode. Fig. S1B displays a STEM image
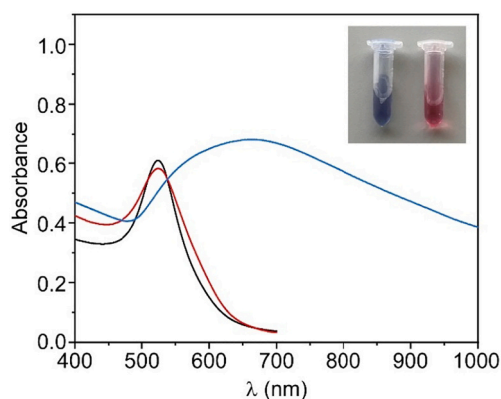
Fig. 1. Absorption spectra of AuNPs synthesized in water (black) and in presence of LUVs of DPPC (blue) and DPPG (red) at 22 °C. Inset: naked eye colours of the solutions of AuNPs in DPPC (left) and DPPG (right). (For interpretation of the references to color in this figure legend, the reader is referred to the web version of this article.)

showing quasi-spherical shapes for AuNPs with particle sizes compatible with those estimated by DLS. To select the most appropriate gold concentration for the synthesis, the concentrations of the metal precursor were varied from 0.05 to 0.5 mM, keeping constant the ascorbic acid concentration at 0.3 mM. Fig. S1A shows that up to a concentration of 0.2 mM of $HAuCl_4$ the shape of the spectrum is preserved, increasing the absorbance signal, suggesting that the nanoparticles maintain the same size, but grow in number. However, at higher concentrations, a red-shift of the absorption maximum was observed, together with a broadening of the spectrum, suggesting that AuNPs either increase in size or change their morphology or aggregate. Based on these results, we selected 0.2 mM $HAuCl_4$ as the most suitable concentration for synthesizing AuNPs throughout this work.

The effect of temperature on the synthesis of AuNPs was explored by comparing the results obtained when performed at 3, 22 and 55 °C. The sample color, absorption spectra as well as the hydrodynamic diameter were quite similar, suggesting that temperature hardly modifies the LSPR of AuNPs synthesized in water, at least in the range studied (Fig. S2 and Table 1). The only difference was that at low temperatures the formation kinetics was slightly slower, as the red coloring appeared a few seconds later than in the samples synthesized at higher temperatures. This result is in agreement with that reported by Luty-Blocho et al. who observed that with increasing temperature, the time of nucleation process shortness and autocatalytic growth of AuNPs runs faster, probably as a result of the acceleration of the reduction reaction of Au(III) with ascorbic acid [30].

Table 1

Hydrodynamic diameter (d_i) of AuNPs generated at various temperatures in water and synthesized *in situ* in the presence of LUVs of DPPC and DPPG.

Sample	T	d1 ± sd (nm)	d2 ± sd (nm)
AuNPs in water	3 °C	34.0 ± 0.6	
	22 °C	32.6 ± 0.8	
	55 °C	40.0 ± 1.7	
DPPC	22 °C	141 ± 3	
AuNPs *in situ* (DPPC)	3 °C	223 ± 7	
	22 °C	205 ± 7	
	55 °C	155 ± 3	
DPPG	22 °C	137 ± 3	
AuNPs *in situ* (DPPG)	22 °C	140 ± 12 (85%)*	20 ± 17 (15%)*

* Population percentage

3.2. In situ synthesis of AuNPs in presence of LUVs

Synthesis of AuNPs was carried out at 22 °C in presence of LUVs of DPPC and DPPG, previously fabricated as described in Materials and Methods. After addition of precursors, the DPPC sample quickly turned blue-violet, while a red color was observed in the DPPG sample. The absorption spectra and photographs (inset) of the solutions are shown in Fig. 1. It can be seen that the sample containing DPPG showed a narrow spectral band with a maximum at ~525 nm, which coincides with the position of the LSPR peak of AuNPs obtained in water. In contrast, for DPPC the absorption spectrum became broader and shifted ~120 nm towards longer wavelengths. Samples were characterized by DLS and results are shown in Table 1. For DPPG, two populations were observed, one with a diameter similar to that of the pure liposomes and the second one with a size comparable to that of AuNPs synthesized in water; while for DPPC, only one population of particles was detected, with a diameter about 60 nm larger than that of the liposomes alone.

The above results suggest that AuNPs are synthesized in both cases but, in the presence of DPPG, they remain suspended in the aqueous solution instead of forming on the liposomes. In contrast, the blue color of the suspension and the position and shape of the LSPR band evidence that when the synthesis is performed in the presence of DPPC, the nanoparticles form on the liposome surface, most likely arranged in aggregates, leading to AuNPs@DPPC nanohybrids.

These results could be explained in part taking into account that the *in situ* synthesis involves electrostatic interactions between the negatively charged AuNPs or their precursors and the positively charged groups of the support. In the case of LUVs composed of DPPG, the negatively charged phosphate group of the lipid is exposed to the aqueous phase, preventing the formation of nanoparticles on their surface due to repulsion between charges. In contrast, for the zwitterionic DPPC, the presence of the cationic ammonium group of choline facilitates the interaction with anionic species, allowing the synthesis of the AuNPs on the membrane surface.

Since DPPG does not prove to be a good support for *in situ* synthesis, we continued the study with DPPC. To assess the extent to which the lipid phase influences the formation and arrangement of AuNPs on the membrane surface, a set of samples of DPPC LUVs were prepared and subjected to a temperature gradient from 0.4 to 70 °C. Once the temperature was equilibrated, precursors were added and, after stirring, color appearance was observed confirming the formation of the AuNPs. Surprisingly, a color scale, ranging from blue-green to red, was observed as the synthesis temperature increased (Fig. 2A). This coloration was maintained when all samples were brought to room temperature and was preserved for several weeks. Absorption spectra of some of these samples are displayed in Fig. 2B. Results show that for AuNPs synthesized around and above the T_m (~42 °C), the color of the samples was red and the position and width of the plasmon band was close to that observed in water. In contrast, below T_m, the samples became increasingly bluish, even turning greenish in appearance at low temperatures and the absorption band broadened, shifting towards the NIR.

Changes in LSPR were better observed when the absorption maximum and Half width at half maximum (HWHM) of the sample spectra were plotted *versus* synthesis temperature. The results show at least two trends (Fig. 2C). If we observe the plot starting from the highest synthesis temperature and going down to T_m, the temperature effect is minimal in both, the peak maximum and the spectral width. Between 42 and ~ 30 °C, a slight red-shift is observed and the band becomes wider. In contrast, for lower temperatures, a marked shift is observed up to around 850 nm, together with a strong broadening of the band, the effect being more pronounced at low temperatures. Note that these values correspond to wavelengths in the first NIR optical window, known as the therapeutic window, where tissue absorption is small compared to scattering [31].

The position and width of the LSPR band around and above T_m, suggest that at these temperatures either AuNPs are formed individually
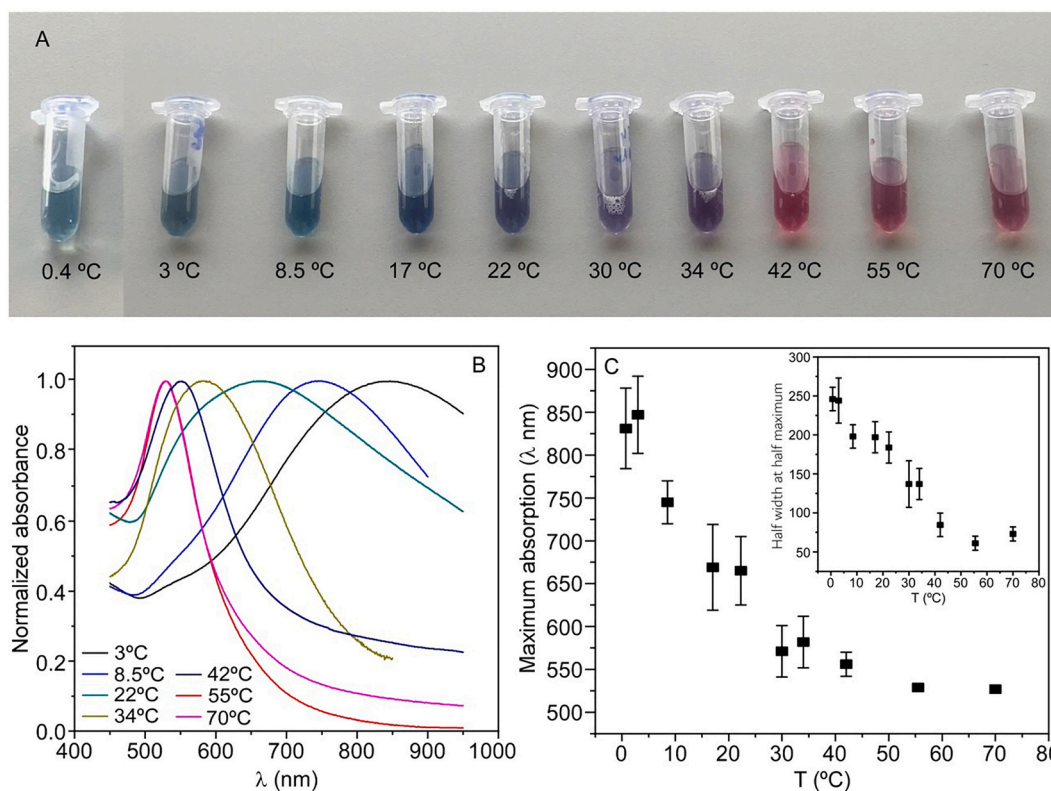
Fig. 2. (A) Photograph of AuNPs synthesized *in situ* in DPPC LUVs at different temperatures. (B) Absorption spectra of the samples in Fig. 2A synthesized at different temperatures. (C) Spectral properties (absorption maximum wavelength and half-width at half maximum -inset-) of the samples displayed in Fig. 2A.

on the membrane surface, or they are synthesized in the aqueous phase, without binding to liposomes. On the contrary, below T_m, AuNPs are synthesized on the lipid bilayer, remaining very close to each other, forming aggregates or clusters whose size seems to increase as the synthesis temperature decreases.

To test this hypothesis, DLS measurements were recorded for a number of selected samples. In all of them, a single population was observed which, in the case of nanohybrids synthesized above T_m, showed a diameter very similar to that of DPPC LUVs. However, the size increased when AuNPs were synthesized at temperatures below T_m: the lower the temperature, the larger the size obtained (Table 1). These results indicate that above T_m, despite retaining the red color and the position of the LSPR band near 525 nm, AuNPs are mostly synthesized on the liposome, probably in isolated form. Results also support the hypothesis that below T_m AuNPs are arranged on the lipid bilayer in clusters or aggregates, whose size and plasmon band can be modulated as a function of the synthesis temperature.

This assumption was confirmed from FESEM-STEM analysis of nanohybrids synthesized at 0.4, 22 and 55 °C. Images in Fig. 3 (left column) evidence the presence of spherical-shaped vesicles on which nanoparticles are located. The EDX spectrum showed Au peaks, denoting the occurrence of gold in the composition of the nanoparticles (Fig. S3). Results confirm that AuNPs synthesized at 55 °C mostly adsorb/bind individually on the lipid bilayers, while they form aggregates localized on the liposome surface when synthesized below T_m. Such aggregates are found in the form of particle nanoclusters arranged in 3-dimensions, rather than surrounding the liposome (Fig. 3, right column). It is interesting to note that at low temperatures the nanoclusters have diameters of 60–80 nm with a quasi-fractal shape and are formed by the assembly of small AuNPs. However, at 22 °C, AuNPs seem to coalesce on the membrane surface forming compact amorphous nanostructures, rather than clusters.

In order to explain these results, we can consider factors such as the

different phases in which DPPC lipids can be arranged as a function of temperature, as well as kinetics factors. For $T < T_m$ at least two phases with ordered hydrocarbon chain arrangements named gel phase ($L_{\beta'}$) and ripple phase ($P_{\beta'}$) have been reported [32]. $L_{\beta'}$ extends from low temperatures to ~33 °C and is characterized by lipid chains extended and packed tightly together, which greatly restrict their mobility. Phase transition between $L_{\beta'}$ and $P_{\beta'}$ (so-called pretransition, T_p) occurs around 33 °C. In $P_{\beta'}$ which extends up to 42 °C, the lipid bilayer is characterized by periodic undulations on the membrane surface that increase the space occupied by lipid polar headgroups. Finally, above T_m lipids are in the fluid phase or $L_{\alpha'}$, where the acyl chains have a substantial degree of conformational disorder and lateral and rotational mobility largely increasing the permeability and degree of hydration of the bilayer relative to the $L_{\beta'}$ phase.

The *Z*-potential is also strongly dependent on the phase state of the lipids. LUVs of DPPC in water have been described by Morini et al. to show a low positive Z-potential in $L_{\beta'}$, which decreases at the onset of pre-transition and becomes negative above T_m, as a consequence of the reorientation of the polar heads and the increase in the degree of hydration [33]. In that work authors suggest that in $L_{\beta'}$ the cationic ammonium group of choline emerges from the membrane plane into the aqueous phase, while the phosphate group remains less exposed, giving the bilayer surface a positive charge. In contrast, below T_p and especially in $L_{\alpha'}$ phase, there is a protrusion of the phosphate group out of the membrane plane towards the aqueous phase, while the choline group remains in a more hydrophobic environment. Given this scenario, it is likely that when synthesis takes place below T_p, the negatively charged precursors tend to bind to the water-exposed ammonium group and the tight packing of the phospholipid chains forces these precursors to remain on the surface, preventing the inclusion of the AuNPs in the lipid bilayer and inducing their aggregation. The reason why the plasmon shifts progressively towards the NIR as the temperature decreases in this range is not clear, but it is probably a consequence of the slowing down
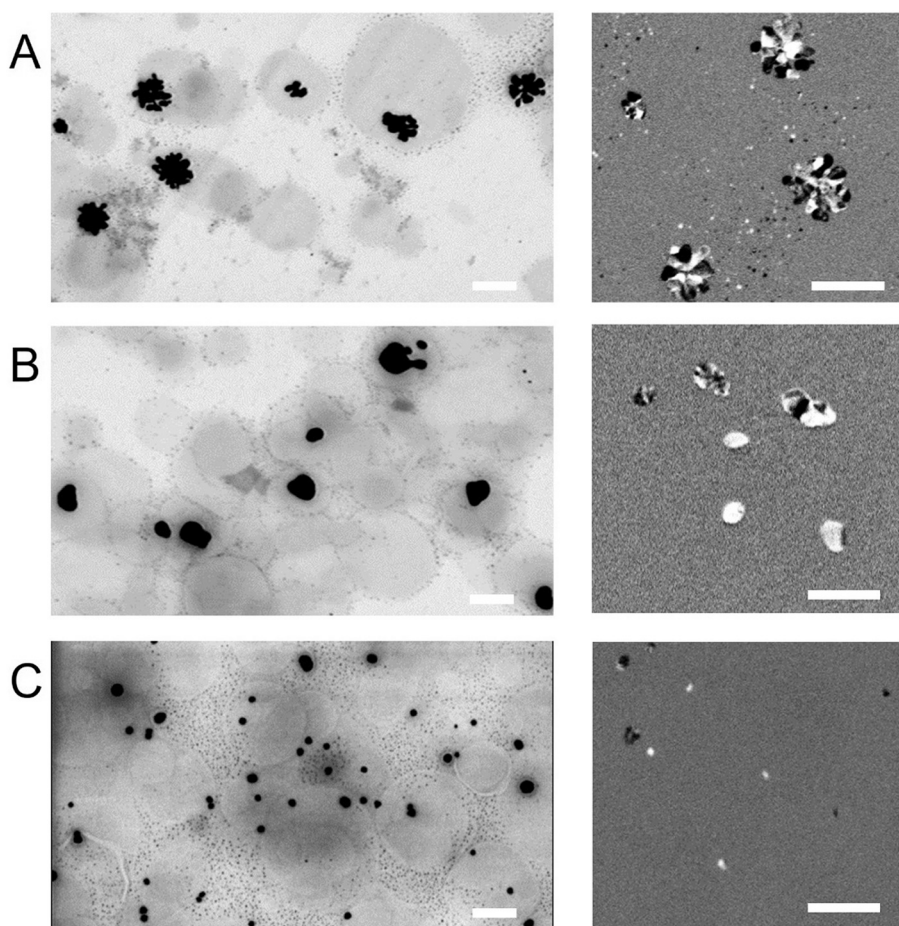
Fig. 3. FESEM-STEM images in BF (left column) and ODF (right column) modes of AuNPs@DPPC nanohybrids synthesized at (A) 0.4 °C, (B) 22 °C and (C) 55 °C (scale bar = 100 nm).

of the synthesis steps and the diffusion rate, combined with increased lipid packing, which causes the aggregates formed to differ in their final arrangement and morphology, as observed in Fig. 3 by FESEM-STEM (left column). Variations in the intensity patterns of the AuNPs, detected by ODF mode (right column), highlight differences in the formed metal nanostructures. Probably, as diffusion is slower at low temperatures, the nascent nanoparticles might not have time to coalesce before being stabilized by the positively charged surface, arranging themselves in the form of nanoclusters. Increasing the temperature will favor the contact between them and their adhesion/coalescence leading to more compact aggregates. On the contrary, when the synthesis is carried out at temperatures above T_p and, especially, above T_m, the increased fluidity of the bilayer will allow the precursors to access the hidden choline groups, facilitating the formation of individual AuNPs. These changes in morphology will significantly affect the interaction of light and thus the spectral position of the LSPR.

This assumption was confirmed from similar experiments performed with DMPC LUVs. This lipid has the same headgroup as DPPC, but T_m = 22 °C. As can be seen in Fig. S4, nanohybrids showed different spectral characteristics depending on the synthesis temperature. At $T \geq 22$ °C, the red color of the sample and the position of the plasmon band were similar to those obtained in DPPC at 42 °C. In contrast, below T_m, the sample turned bluish-greenish and the absorption maximum shifted to ~835 nm at 14 °C. The size of the nanohybrids was also modified as a function of the synthesis temperature. While at 50 °C the hydrodynamic diameter was 128.2 ± 0.5 nm, similar to that of DMPC LUVs (127.5 ± 0.7), at 14 °C it increased to 191.1 ± 0.7 nm. Although these results confirm our hypothesis, it is noteworthy that at low temperatures

nanohybrids exhibited a much flatter spectrum with very low absorbance, probably because DMPC LUVs have a more negative Z-potential than DPPC LUVs [33], due to the choline headgroup being less exposed to water, making this lipid less suitable as a support for *in situ* AuNPs synthesis.

3.3. Stability and physical properties of nanohybrids

The stability of nanohybrids synthesized at 22 °C (AuNP@DPPC_22) and 55 °C (AuNP@DPPC_55) was explored as a function of time by measuring the evolution of their hydrodynamic diameters, Z potential (pZ) and absorption spectra for 35–40 days after being stored at 4 °C (Fig. S5). The results confirm that both systems retained their size, surface charge and plasmon position during this period. Furthermore, since only a single population and no significant variation in pZ values was observed, it was concluded that AuNPs, both in aggregate and isolated form, remain attached to the vesicles throughout this time.

The effect of gold nanoparticles on the physical properties of the bilayer was explored by measuring the steady-state fluorescence anisotropy <r > and the fluorescence lifetimes of the membrane probe DPH. This fluorophore is incorporated into the bilayer, mainly parallel to the lipid chains, and its steady-state anisotropy and fluorescence lifetime values provide information on the membrane order (fluidity) and degree of hydration of the most hydrophobic region of the bilayer, respectively [34,35]. The more fluid the bilayer, the lower the anisotropy value, and the higher the water content, the shorter the lifetime. Measurements were performed at 25, 38 and 50 °C on DPPC LUVs and nanohybrids synthesized at 0.4 °C (AuNP@DPPC_0) and 55 °C (AuNP@DPPC_55)

(AuNP@DPPC_55). $<r>$ was calculated using Eq. S1, while the fluorescence profiles were fitted to a double exponential decay model (Fig. S6) and the mean fluorescence lifetime $<\tau>$ was calculated from this fit using Eq. S2. The results are shown in Table 2. As was expected for pure DPPC, high values of $<r>$ and $<\tau>$ were found at 25 °C, as a consequence of the high lipid packing of the L_{β}' phase that hinders the movement of the probe and water penetration. The $<r>$ values slightly decreased in the ripple phase, and much more strongly above T_m, evidencing the abrupt increase in the conformational freedom of the lipid chains, which takes place in the L_{α}' phase allowing the probe tumbling and its concomitant fluorescence emission depolarization. The $<\tau>$ value also dropped up to 8.2 ns at temperatures above T_m, mainly as consequence of the increase in the polarity of the medium due to the higher penetration of water molecules into the membrane, which quench the fluorescence of DPH [36,37]. Results in Table 2 show that the AuNP@DPPC_0 and AuNP@DPPC_55 nanohybrids exhibited values of $<r>$ and $<\tau>$ similar to those obtained in pure DPPC for the three temperatures explored, evidencing that AuNPs, whether synthesized as aggregates or individually, are located on the surface and not in the hydrophobic core of the bilayer, without disturbing either the fluidity or the degree of hydration.

Finally, the thermotropic behavior of the nanohybrids was explored measuring the $<r>$ of DPH as a function of temperature. As is shown in Fig. 4, a sharp drop of the anisotropy was observed around 42 °C for liposomes in absence of AuNPs, confirming that lipids undergo phase transition cooperatively. In the nanohybrids the anisotropy showed a similar drop, although very slightly shifted towards higher temperatures. From the first derivative of these curves, the T_m value for each sample was determined (inset in Fig. 4). No further relevant differences were observed, neither in structural order ($<r>$ values) nor in thermal behavior (cooperativity of the process). Thus, the presence of AuNPs in DPPC, either as nanoclusters or individually arranged, would only increase the transition temperature of the liposomes by 1 °C, preserving their integrity. This small increase in the T_m value may be due to the fact that the electrostatic interactions between the AuNPs and the membrane surface cause the repulsions of the lipid headgroups to be shielded. Consequently, more favourable chain-chain interactions and thus a slight stabilization of the gel phase with respect to the fluid phase can be expected.
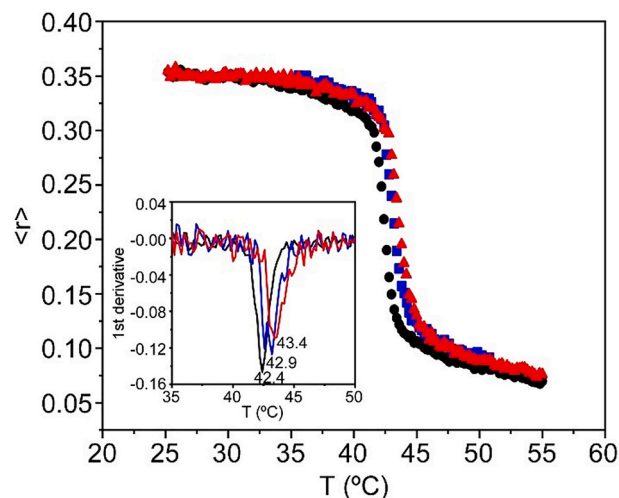
3.4. Photothermal properties of nanohybrids

Experimental studies were carried out to demonstrate the potential application of the AuNPs@DPPC nanohybrids as photothermal agents, able to generate heat when irradiated with NIR light. For this purpose, a continuous wave laser at 1064 nm was employed, as is described in Materials and Methods to irradiate nanohybrids synthetized at 0.4, 30 and 55 °C (AuNP@DPPC_0, AuNP@DPPC_30, AuNP@DPPC_55, respectively). Laser irradiation with different power densities were tested as a function of time. A solution devoid of nanohybrids (water-only sample) was used as control for each experiment. As shown in Figs. 5, the higher the laser power density, the higher the temperature
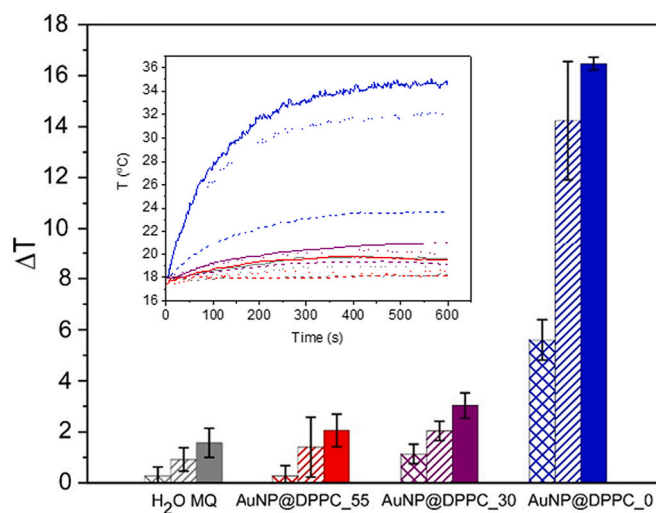

Fig. 4. Anisotropy values, $<r>$, of DPH as a function of temperature in DPPC LUVs (black circles) and nanohybrids; AuNP@DPPC_0 (blue squares) and AuNP@DPPC_55 (red triangles). Inset: First derivative of the anisotropy. (For interpretation of the references to color in this figure legend, the reader is referred to the web version of this article.)

Fig. 5. Temperature change induced by different power densities: 1.44 (sparse), 2.94 (striped) and 5.84 W/cm^2 (solid), ($\lambda = 1064$ nm, irradiation time 10 min) on a water sample (gray) and AuNP@DPPC_55 (red), AuNP@DPPC_30 (purple), and AuNP@DPPC_0 (blue) nanohybrid suspensions. The increment was calculated from the photothermal curves shown in the Inset. (For interpretation of the references to color in this figure legend, the reader is referred to the web version of this article.)

increase and, the longer the irradiation time, the higher the temperature achieved, until a plateau is reached (inset in Fig. 5). NIR irradiation for 10 min of a sample containing AuNP@DPPC_0, induced a temperature rise of up to 16 °C, depending on the laser power density. In sharp contrast, irradiation of AuNP@DPPC_30 only increased by about 3 °C the sample temperature, while for those made at 55 °C, the effect was similar to that occurring when water was irradiated. Therefore, results confirm the potential use of nanohybrids as photothermal agents and reveal that those fabricated at low temperatures are capable of greatly raising the sample temperature when irradiated at NIR wavelength due to the position of the LSPR band. This increment is sufficient to trigger the gel-fluid phase transition in thermosensitive liposomes that are locally irradiated at physiological temperatures, as well as to induce cell damage. Lasers with shorter wavelengths, in the visible region, would be

Table 2
Steady state anisotropy $<r>$ and mean lifetime $<\tau>$ of DPH in DPPC LUVs and nanohybrids synthesized at 0.4 °C (AuNP@DPPC_0) and 55 °C (AuNP@DPPC_55).

T (°C)	DPPC		AuNP@DPPC_55		AuNP@DPPC_0	
	$<r>$	$<\tau>$ (ns)	$<r>$	$<\tau>$ (ns)	$<r>$	$<\tau>$ (ns)
25	0.351 ± 0.005	11.22 ± 0.03	0.353 ± 0.005	11.14 ± 0.04	0.354 ± 0.005	11.24 ± 0.11
38	0.328 ± 0.005	11.21 ± 0.04	0.336 ± 0.005	11.16 ± 0.03	0.335 ± 0.005	11.23 ± 0.03
50	0.088 ± 0.005	8.19 ± 0.02	0.081 ± 0.005	8.20 ± 0.02	0.086 ± 0.005	8.24 ± 0.02

needed to excite the nanohybrids that have been synthesized at higher temperatures, in order to exploit their photothermal effects.

4. Conclusions

Stable AuNPs@DPPC nanohybrids with on-demand plasmon mode and good photothermal conversion efficiency have been successfully developed using an effective, low cost and environmentally friendly methodology in which AuNPs are easily and rapidly synthesized *in situ* on the surface of DPPC thermosensitive liposomes exposed at different temperatures. Both the lipid phase and temperature influence the final arrangement of the AuNPs, so aggregation is inhibited when the synthesis is performed in fluid phase, resulting in discrete AuNPs with LSPR in the visible region, and promoted when the membrane is in gel phase, giving rise to plasmon bands progressively more shifted towards the NIR as the synthesis temperature decreases. Such aggregates are found in the form of AuNPs nanoclusters with quasi-fractal shapes that tend to coalesce as the synthesis temperature rises.

The AuNPs@DPPC nanohybrids retain the physical properties of the DPPC liposomes, without altering either the fluidity or the degree of hydration of the bilayer, and only a very slight shift towards higher temperatures in the T_m value is observed, remaining within mild-hyperthermia range and evidencing that the integrity of the liposome is preserved. Furthermore, AuNPs@DPPC nanohybrids synthesized at low temperatures showed good light-to-heat conversion properties when irradiated in the near-infrared, which warrants promising applications in light-mediated therapies such as NIR light-controlled drug delivery and NIR light-mediated photothermal and photodynamic therapies. In addition to therapeutical applications, since LSPR of gold nanoparticles can be lead to surface-enhanced Raman spectroscopy, surface enhanced fluorescence, photochemical conversion, enhanced photoacoustic, enhanced catalysis and colorimetric responses, we believe that the possibility to easily control and tune the plasmon modes of the developed nanohybrids within the VIS/NIR region will also be of interest to a wide spectrum of researchers working in in other fields such as nanophotonics, optical sensing, catalysis or imaging.

Declaration of Competing Interest

The authors declare that they have no known competing financial interests or personal relationships that could have appeared to influence the work reported in this paper.

Data availability

Data will be made available on request.

Acknowledgements

Appendix A. Supplementary data

Supplementary data to this article can be found online at https://doi.org/10.1016/j.colcom.2022.100690.

References

[1] X. Huang, M.A. El-Sayed, Gold nanoparticles: optical properties and implementations in cancer diagnosis and photothermal therapy, J. Adv. Res. 1 (2010) 13–28.

[2] D. Cabuzu, A. Cirja, R. Puiu, A.M. Grumezescu, Biomedical applications of gold nanoparticles, Curr. Top. Med. Chem. 15 (2015) 1605–1613.

[3] J. Liu, H. He, D. Xiao, S. Yin, W. Ji, S. Jiang, D. Luo, B. Wang, Y. Liu, Recent advances of plasmonic nanoparticles and their applications, Mater 11 (2018) 1833.

[4] F. Duarte, J.P.N. Torres, A. Baptista, R.A. Marques Lameirinhas, Optical nanoantennas for photovoltaic applications, Nanomater 11 (2021) 422.

[5] S. Haque, C.R. Patra, Biologically synthesized gold nanoparticles as a near-infrared-based bioimaging agent, Nanomedicine (London) 16 (2021) 1–4.

[6] C.C. Chang, C.P. Chen, T.H. Wu, C.H. Yang, C.W. Lin, C.Y. Chen, Gold nanoparticle-based colorimetric strategies for chemical and biological sensing applications, Nanomater 9 (2019) 861.

[7] B. Sharma, R.R. Frontiera, A.I. Henry, E. Ringe, R.P. Van Duyne, SERS: materials, applications, and the future, Mater. Today 15 (2012) 16–25.

[8] J.B. Vines, J.H. Yoon, N.E. Ryu, D.J. Lim, H. Park, Gold nanoparticles for photothermal cancer therapy, Front. Chem. 7 (2019) 167.

[9] X. Huang, M.A. El-Sayed, Plasmonic photo-thermal therapy (PPTT), Alexandria J. Med. 47 (2011) 1–9.

[10] M. Pérez-Hernández, P. Del Pino, S.G. Mitchell, M. Moros, G. Stepien, B. Pelaz, W. J. Parak, E.M. Gálvez, J. Pardo, J.M. De La Fuente, Dissecting the molecular mechanism of apoptosis during photothermal therapy using gold nanoprisms, ACS Nano 9 (2015) 52–61.

[11] X. Jiang, R. Liu, P. Tang, W. Li, H. Zhong, Z. Zhou, J. Zhou, Controllably tuning the near-infrared plasmonic modes of gold nanoplates for enhanced optical coherence imaging and photothermal therapy, RSC Adv. 5 (2015) 80709–80718.

[12] S. Lee, K. Sim, S.Y. Moon, J. Choi, Y. Jeon, J.-M. Nam, S.-J. Park, S. Lee, S.Y. Moon, J. Choi, Y. Jeon, S.-J. Park, K. Sim, J.-M. Nam, Controlled assembly of plasmonic nanoparticles: from static to dynamic nanostructures, Adv. Mater. 33 (2021) 2007668.

[13] L.L. Félix, J.M. Porcel, F.F.H. Aragón, D.G. Pacheco-Salazar, M.H. Sousa, Simple synthesis of gold-decorated silica nanoparticles by in situ precipitation method with new plasmonic properties, SN Appl. Sci. 3 (2021) 1–10.

[14] J.E. Ortiz-Castillo, R.C. Gallo-Villanueva, M.J. Madou, V.H. Perez-Gonzalez, Anisotropic gold nanoparticles: a survey of recent synthetic methodologies, Coord. Chem. Rev. 425 (2020), 213489.

[15] B. Pelaz, V. Grazu, A. Ibarra, C. Magen, P. Del Pino, J.M. De La Fuente, Tailoring the synthesis and heating ability of gold nanoprisms for bioapplications, Langmuir 28 (2012) 8965–8970.

[16] S. Bhaskar, R. Patra, N.C.S.S. Kowshik, K.M. Ganesh, V. Srinivasan, P. Chandran, S. S. Ramamurthy, Nanostructure effect on quenching and dequenching of quantum emitters on surface plasmon-coupled interface: a comparative analysis using gold nanospheres and nanostars, Phys. E Low-Dimension Syst. Nanostruct. 124 (2020), 114276.

[17] J.E. Millstone, S. Park, K.L. Shuford, L. Qin, G.C. Schatz, C.A. Mirkin, Observation of a quadrupole plasmon mode for a colloidal solution of gold nanoprisms, J. Am. Chem. Soc. 127 (2005) 5312–5313.

[18] A. Rai, S. Bhaskar, N. Reddy, S.S. Ramamurthy, Cellphone-aided attomolar zinc ion detection using silkworm protein-based nanointerface engineering in a plasmon-coupled dequenched emission platform, ACS Sustain. Chem. Eng. 9 (2021) 14959–14974.

[19] S. Bhaskar, A. Rai, K.M. Ganesh, R. Reddy, N. Reddy, S.S. Ramamurthy, Sericin-based bio-inspired nano-engineering of heterometallic AgAu nanocubes for attomolar mefenamic acid sensing in the mobile phone-based surface plasmon-coupled interface, Langmuir 38 (2022) 12035–12049.

[20] A. Rai, S. Bhaskar, K.M. Ganesh, S.S. Ramamurthy, Hottest hotspots from the coldest cold: welcome to Nano 40, ACS Appl. Nano Mater. 5 (2022) 12245–12264.

[21] S.K. Ghosh, T. Pal, Interparticle coupling effect on the surface plasmon resonance of gold nanoparticles: from theory to applications, Chem. Rev. 107 (2007) 4797–4862.

[22] C. Daruich De Souza, B. Ribeiro Nogueira, M.E.C.M. Rostelato, Review of the methodologies used in the synthesis gold nanoparticles by chemical reduction, J. Alloys Compd. 798 (2019) 714–740.

[23] R. Li, X. Gu, X. Liang, S. Hou, D. Hu, Aggregation of gold nanoparticles caused in two different ways involved in 4-mercaptophenylboronic acidand hydrogen peroxide, Mater 12 (2019) 1802.

[24] L. Amornkitbamrung, J. Kim, Y. Roh, S.H. Chun, J.S. Yuk, S.W. Shin, B.W. Kim, B. K. Oh, S.H. Um, Cationic surfactant-induced formation of uniform gold nanoparticle clusters with high efficiency of photothermal conversion under near-infrared irradiation, Langmuir 34 (2018) 2774–2783.

[25] J. Michael Köhler, J. Kluitmann, In situ assembly of gold nanoparticles in the presence of poly-DADMAC resulting in hierarchical and highly fractal nanostructures, Appl. Sci. 11 (2021) 1191.

[26] T.S. Troutman, S.J. Leung, M. Romanowski, M. Romanowski, T.S. Troutman, S. J. Leung, Light-induced content release from plasmon-resonant liposomes, Adv. Mater. 21 (2009) 2334–2338.

[27] T.K. Sau, A.S. Urban, S.K. Dondapati, M. Fedoruk, M.R. Horton, A.L. Rogach, F. D. Stefani, J.O. Rädler, J. Feldmann, Controlling loading and optical properties of gold nanoparticles on liposome membranes, Colloids Surf. A Physicochem. Eng. Asp. 342 (2009) 92–96.

[28] M. Rubio-Camacho, Y. Alacid, R. Mallavia, M.J. Martínez-Tomé, C.R. Mateo, Polyfluorene-based multicolor fluorescent nanoparticles activated by temperature for bioimaging and drug delivery, Nanomater. 9 (2019) 1485.

[29] M. Amin, W. Huang, A.L.B. Seynhaeve, T.L.M. Ten Hagen, Hyperthermia and temperature-sensitive nanomaterials for spatiotemporal drug delivery to solid tumors, Pharmaceutics 12 (2020) 1007.

[30] M. Luty-Błocho, M. Wojnicki, K. Fitzner, Gold nanoparticles formation via Au(III) complex ions reduction with L-ascorbic acid, Int. J. Chem. Kinet. 49 (2017) 789–797.

[31] L.A. Sordillo, Y. Pu, S. Pratavieira, Y. Budansky, R.R. Alfano, Deep optical imaging of tissue using the second and third near-infrared spectral windows, J. Biomed. Opt. 19 (2014), 056004.

[32] S. Nagarajan, E.E. Schuler, K. Ma, J.T. Kindt, R.B. Dyer, Dynamics of the gel to fluid phase transformation in unilamellar DPPC vesicles, J. Phys. Chem. B 116 (2012) 13749–13756.

[33] M.A. Morini, M.B. Sierra, V.I. Pedroni, L.M. Alarcon, G.A. Appignanesi, E. A. Disalvo, Influence of temperature, anions and size distribution on the zeta potential of DMPC, DPPC and DMPE lipid vesicles, Colloids Surf. B: Biointerfaces 131 (2015) 54–58.

[34] R. Esquembre, M.L. Ferrer, M.C. Gutiérrez, R. Mallavia, C.R. Mateo, Fluorescence study of the fluidity and cooperativity of the phase transitions of zwitterionic and anionic liposomes confined in sol-gel glasses, J. Phys. Chem. B 111 (2007) 3665–3673.

[35] L.F. Aguilar, J.A. Pino, M.A. Soto-Arriaza, F.J. Cuevas, S. Sánchez, C.P. Sotomayor, Differential dynamic and structural behavior of lipid-cholesterol domains in model membranes, PLoS One 7 (2012), e40254.

[36] R. Fiorini, M. Valentino, S. Wang, M. Glaser, E. Gratton, Fluorescence lifetime distributions of 1,6-diphenyl-1,3,5-hexatriene in phospholipid vesicles, Biochemistry 26 (1987) 3864–3870.

[37] C. Bernsdorff, A. Wolf, R. Winter, E. Gratton, Effect of hydrostatic pressure on water penetration and rotational dynamics in phospholipid-cholesterol bilayers, Biophys. J. 72 (1997) 1264–1277.